JOURNAL OF MATERIALS SCIENCE 23 (1988) 1385–1390

Control of the continuous rheocasting process

Part 2 *Rheological behaviour analysis*

M. A. TAHA, N. A. EL-MAHALLAWY, A. M. ASSAR
Department of Mechanical Design and Production Engineering, Faculty of Engineering, Ain Shams University, Abasia, Cairo, Egypt

The flow rate at the exit port of a continuous rheocaster is dependent on the viscosity of the semi-solid slurry. Slurry viscosity can be determined by the shear rate induced in the stirring chamber and the solid volume fraction attained at the exit port. For this purpose, an analytical study is made on the rheological behaviour and slurry flow rate of Bi–17 wt% Sn alloy in a continuous rheocaster. The rheological equation of state needed for such study is obtained by using measured slurry flow curves.

Nomenclature

g	Gravity acceleration ($m\,sec^{-2}$)
G_s	Volume fraction of solid
h	Height of the slurry in the stirring chamber (m)
L	Height of the stirring chamber (m)
M_1	Measured torque (N m)
M	Steady-state torque (N m)
P	Static pressure ($N\,m^{-2}$)
P_0	Static pressure at the end of the stirring chamber ($N\,m^{-2}$)
P_h	Static pressure at the beginning of the stirring chamber ($N\,m^{-2}$)
Q_m	Maximum theoretical flow rate ($kg\,sec^{-1}$)
Q_p	Experimental flow rate at the exit port ($kg\,sec^{-1}$)
r	Radial coordinate (m)
R_1	Stirrer radius (m)
R_2	Inner radius of the stirring chamber (m)
S_v	Solid–liquid interface area per unit volume of solid (m^{-1})
T	Temperature (K)
V_r	Velocity component in radial direction ($m\,sec^{-1}$)
V_θ	Velocity component in angular direction ($m\,sec^{-1}$)
V_z	Velocity component in axial direction, ($m\,sec^{-1}$)
$\bar{V}_z$	Average velocity component in axial direction ($m\,sec^{-1}$)
ω_i	Angular velocity (sec^{-1})
z	Axial coordinate (m)
ϱ	Specific gravity ($kg\,m^{-3}$)
η_a	Apparent viscosity ($N\,sec\,m^{-2}$)
η_0	Dynamic viscosity of liquid metal ($N\,sec\,m^{-2}$)
η_r	Relative viscosity
γ	Average shear rate (sec^{-1})
τ	Shear stress ($N\,m^{-2}$)
τ_i	Shear stress at radius R_1 ($N\,m^{-2}$)
τ_0	Shear stress at radius R_2 ($N\,m^{-2}$)
λ_m	Average solid particle size (μm)

1. Introduction

In the continuous rheocasting technique, a continuous flow of partially solidified alloy is produced at the exit port of the continuous rheocaster after being vigorously agitated while flowing in a vertical chamber with negative temperature gradient. The process has given several indications of improvements and/or modifications in structure, soundness, homogeneity, physical properties, formability and even machinability of the rheocast products [1–15]. However, the application of the process is still limited, partially due to the difficulty in controlling the process parameters. The temperature distribution along the rheocaster is a very important parameter as it affects the solid fraction at the exit port. The relationship between the design of the rheocaster and the temperature distribution has been treated in another paper [16]. The rheological behaviour of the slurry as it flows along the rheocaster and from the exit port is another important parameter in the process. The latter is analysed in the present work. It includes relationships between the viscosity and the volume fraction of solid, the shear rate and the slurry flow rate. Previous studies on the rheological behaviour of rheocast slurries were made on a batch-type rheocaster (used as a viscometer) where the viscosity–shear rate relationship [6] or the fluidity–structure relationship were experimentally investigated [8, 17]. In the present work, the Bi–17 wt % Sn alloy is considered as a model system.

2. Experimental set-up and procedure

A continuous rheocaster is used in this work as shown in Fig. 1. It consists of an upper cylindrical crucible where the metal alloy is molten and held at a constant temperature using resistance coils. The stirring chamber, located below the crucible, consists of a cylindrical stirrer coaxial with the internal chamber wall leaving a gap of 2 mm. A temperature gradient is set up along the stirring chamber using heating and cooling coils around it. This gradient will determine the alloy temperature at the exit port situated at the bottom of the chamber, and hence the volume fraction of solid in the slurry produced. The metal flow through this port is controlled by the vertical position

0022–2461/88 $03.00 + .12

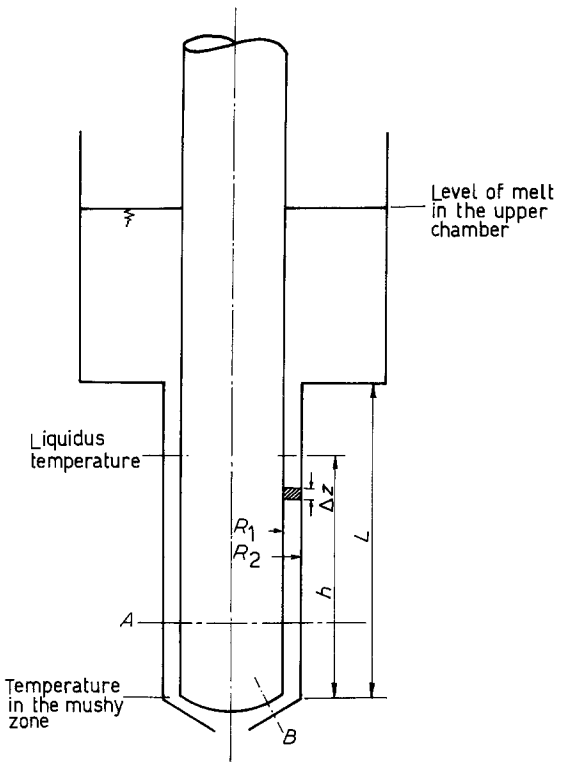

Figure 1 Schematic representation of the continuous rheocaster. $R_1 = 0.0178\,m$, $R_2 = 0.0198\,m$, $L = 0.019\,m$.

of the stirrer. The stirrer is connected to a 1.8 kW, 3000 r.p.m. d.c. motor attached to a speed control unit to achieve a constant speed in case of variations in torque. The Bi–17 wt % Sn alloy used solidifies gradually during its downward flow in the stirring chamber while the slurry is continuously produced due to the stirrer agitation.

The rheocaster was used, at the beginning of the study, as a viscometer and the steady-state torque M acting on the slurry was determined by measuring the current I and by using the experimentally derived relationship

$$M = 0.4\,I$$

where I is the current in amperes.

The shear stress τ can be calculated from the torque, M, the radius of the stirrer, R_1, and the height of the slurry contained in the stirring chamber ($L = 0.19\,m$) using the relationship

$$\tau = M/(2\pi R_1^2 L)$$

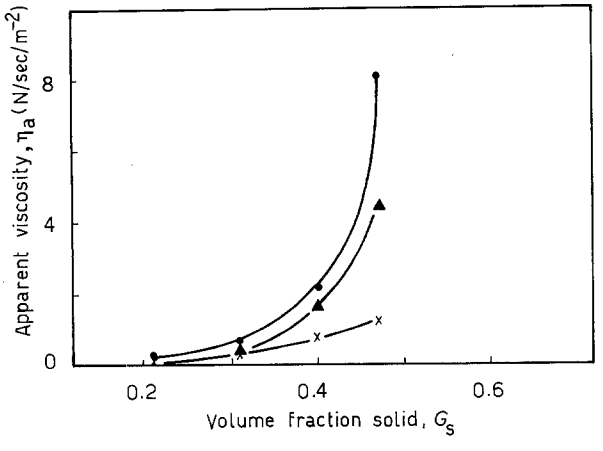

Figure 2 Effect of volume fraction of solid on the apparent viscosity at different values of γ: (●) 200, (▲) 500, (x) 900 sec^{-1}.

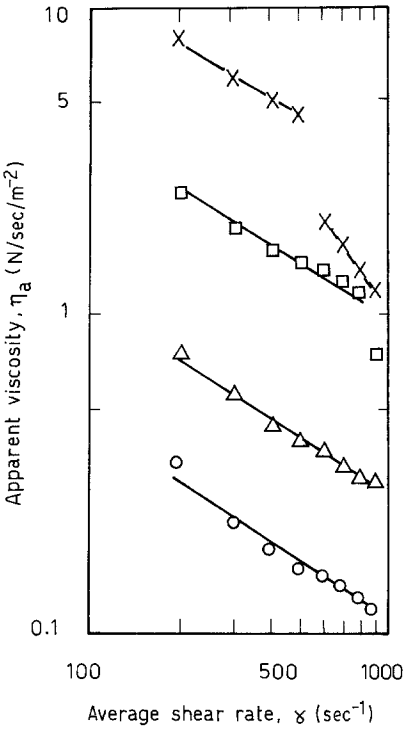

Figure 3 Effect of average shear rate on steady-state apparent viscosity; samples were sheared continuously and held isothermally at different values of G_s (log–log plot). G_s = (○) 0.21, (△) 0.31, (□) 0.40, (x) 0.47.

3. Flow curves and the τ–G_s relationship

The flow curves, which represent the relationship between the shear stress τ and the shear rate γ, are obtained experimentally for the rheocase slurry by using the continuous rheocaster as a viscometer. The following relationship for non-Newtonian suspensions [6, 18, 19] is applied:

$$\tau = \eta_a \gamma \qquad (1)$$

in order to deduce the value of the apparent viscosity η_a, which depends on both γ and on the volume fraction of solid G_s. The value of G_s is determined at any temperature in the mushy zone using the equilibrium diagram as follows [16]:

$$G_s = \frac{1 - 48.5}{261.5 - T} \qquad (2)$$

Fig. 2 shows the relationship between η_a and G_s (0.2 to 0.47) for different γ values. Fig. 3 shows on a log–log scale the η_a–γ relationship where a set of parallel lines are obtained for G_s equal to 0.21 to 0.4. At $G_s = 0.47$, a discontinuity in the line is found at $\gamma = 500$ to $600\,sec^{-1}$.

The relationship between η_a and γ at G_s up to 0.4 is then given by

$$\eta_a = K\gamma^{-0.6} \qquad (3)$$

which is the classical power-law equation used to describe the flow behaviour of shear-rate-dependent materials, with a negative exponent for pseudo-plastic materials [14]. Substituting in Equation 1, the following relationship is obtained

$$\tau = K\gamma^n \qquad (4)$$

where $n = 0.4$.

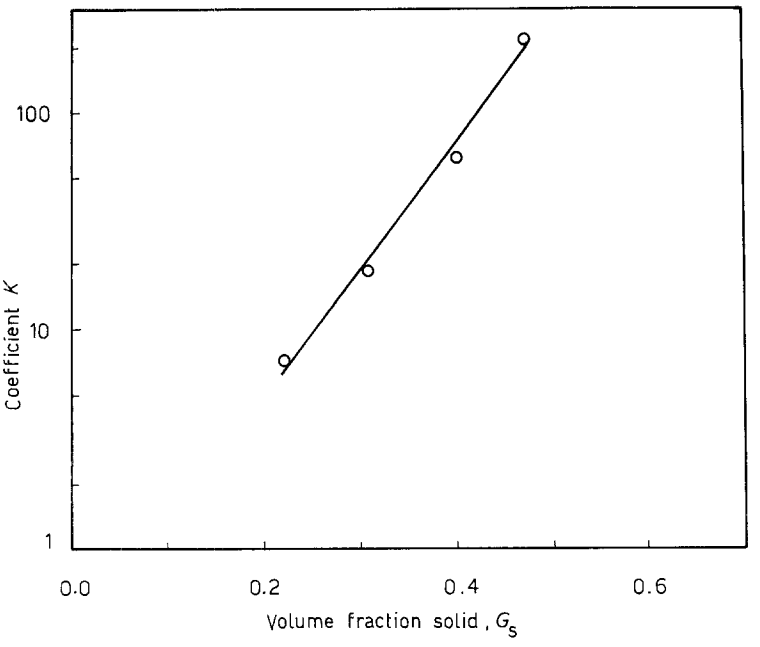

Figure 4 Coefficient K against volume fraction of solid (semi-log plot).

As K is a function of G_s the value of K was plotted against G_s on a semi-log scale (Fig. 4) and the following function obtained:

$$K = 0.34 \exp (13.08\ G_s)$$

By substituting in Equation 3, then

$$\eta_a = 0.34 \exp (13.08\ G_s)\ \gamma^{-0.6} \quad (5)$$

and by susbtituting in Equation 1 the shear stress is given by

$$\tau = 0.34 \exp (13.08\ G_s)\ \gamma^{0.4} \quad (6)$$

4. Torque evaluation

The torque M acting on the stirrer was analysed as in the Appendix and the relationships for G_s and temperature distribution along the stirring chamber were used so that M is described by the semi-empirical equation

$$M = 1.92 \times 10^{-3} (\omega_i)^n \times \int_0^h \exp [13.08\ Sz/(48.5 + Sz)]\ dz \quad (7)$$

where S is the slope defined in the Appendix. This relation estimates the torque at any stirring speed ω_i for a given rheocaster temperature distribution. Computed and experimentally measured torques are given in Table I for different shear rates, where a very good agreement is found between both values.

From Equation A9 in the Appendix and Equation 5,

$$M = 1.92 \times 10^{-3}\ \omega_i^n \int_0^h (1/0.34)\ \eta_a\ \gamma^{0.6}\ dz$$

$$M = 5.65 \times 10^{-3}\ \omega_i^n\ \gamma^{0.6} \int_0^h \eta_a\ dz \quad (8)$$

The relation between rotational speed ω_i and the average shear rate γ, induced in the fluid in the very narrow gap between the stirrer and the stirring chamber, is given [20] as

$$(\gamma = 2\omega_i\ b/(1 - b^2)$$

where $b = R_1/R_2$. Then

$$M = 5.65 \times 10^{-3}\ \omega_i^n \left(\frac{2\omega_i b}{1 - b^2}\right)^{0.6} \int_0^\eta \eta_a\ dz$$

$$M = 8.56 \times 10^{-3}\ \omega_i \left(\frac{b}{1 - b^2}\right)^{0.6} \int_0^h \eta_a\ dz$$

i.e.

$$M = \text{Const.} \times \omega_i \left(\frac{b}{1 - b^2}\right)^{0.6} \int_0^h \eta_a\ dz \quad (9)$$

which describe the torque as function of the stirring speed, the gap width and the apparent viscosity along the stirring chamber.

5. Flow rate in continuous rheocasting

5.1. Mathematical analysis of flow rate–viscosity relationship

The equation of motion is applied to calculate the average velocity of the slurry in the axial direction in the gap between the stirrer and the inner surface of the stirring chamber (Fig. 1). The following assumptions

TABLE I Semi-empirical torque, M, and experimental torque, M_1, for two different stirring conditions

γ (sec^{-1})	Q_p $\times 10^{-3}$ (kg sec^{-1})	G_s (%) (exit)	M (N cm)	M_1 (N cm)
270	12.65	0.15	0.19	0.21
270	11.15	0.22	0.34	0.33
270	8.35	0.27	1.19	1.10
270	7.70	0.30	1.13	1.15
270	6.68	0.32	1.37	1.36
270	6.06	0.35	2.39	2.45
270	5.65	0.38	3.01	3.13
450	13.30	0.14	0.22	0.21
450	9.70	0.26	0.91	1.02
450	8.57	0.31	1.49	1.61
450	7.00	0.35	2.67	2.80
450	6.20	0.37	2.78	2.84
450	5.67	0.40	5.48	5.34
450	4.62	0.43	9.14	9.37

are considered:

(i) The slurry is considered to be an incompressible fluid.

(ii) There is no pressure gradient in the angular direction θ.

(iii) As the density of the solid and liquid phases are almost equal ($9.9 \times 10^3\,kg\,m^{-3}$ for the liquid and $9.35 \times 10^3\,kg\,m^{-3}$ for the solid), it is assumed that the density is uniform along the axial direction.

(iv) Steady-state laminar flow is considered and the velocity component of the slurry in the radial direction, V_r, is zero. The velocity component in the angular direction, V_θ, and in the axial direction, V_z, will be dependent only on the radius r [21].

For this system the well-known equation of motion could be reduced to

$$r \text{ component} \qquad \frac{-/V_\theta^2}{r} = -\frac{dP}{dr} \tag{10}$$

$$\theta \text{ component} \qquad 0 = d\left[\frac{1}{r}\left(\frac{d(rV_\theta)}{dr}\right)\right]\Big/dr \tag{11}$$

$$z \text{ component} \qquad 0 = -\frac{dP}{dz} + \varrho g + \eta_a\left(\frac{1}{r}\right)\left(\frac{d(r\,dV_z/dr)}{dr}\right) \tag{12}$$

Referring to Fig. 1, the boundary conditions can be written as follows:

(a) at $r = R_1$, $V_\theta = \omega_i R_1$ and $V_z = 0$

(b) at $r = R_2$, $V_\theta = 0$ and $V_z = 0$

The solution of Equations 11 and 12 can be written as follows:

$$V_z = \left(\frac{(P_0 - P_h)\,R_2^2}{4\eta_a L}\right)\left\{\left[1 - \left(\frac{r}{R_2}\right)^2\right] + \left[1 - \left(\frac{R_1}{R_2}\right)^2\right]\left(\frac{\ln(r/R_2)}{\ln(R_2/R_1)}\right)\right\} \tag{13}$$

The average velocity in the z direction, $\bar{V}_z$, is obtained from the integration

$$\bar{V}_z = \frac{\int_{R_1}^{R_2} V_z r\,dr}{\int_{R_1}^{R_2} r\,dr}$$

so that

$$\bar{V}_z = \left(\frac{(P_0 - P_h)\,R_2^2}{8\,\eta_a L}\right)\left(\frac{1 - b^4}{1 - b^2} - \frac{1 - b^2}{\ln(1/b)}\right) \tag{14}$$

For the case of constant melt level in the upper chamber during the experiment, then

$$P_0 - P_h = \varrho\,g\,L \tag{15}$$

Substituting from Equation 15 in Equation 14, then

$$\bar{V}_z = \left(\frac{\varrho\,g\,R_2^2}{8\,\eta_a}\right)\left(\frac{1 - b^4}{1 - b^2} - \frac{1 - b^2}{\ln(1/b)}\right) \tag{16}$$

The rate of mass flow Q_m in the z direction is then obtained by multiplying the gap cross-sectional area by the density and $\bar{V}_z$, and is given by

$$Q_m = \text{Gap cross-sectional area} \times \varrho\,\bar{V}_z = \pi R_2^2\left(1 - \frac{R_1^2}{R_2^2}\right)\varrho\,\bar{V}_z$$

$$Q_m = \left(\frac{\pi\varrho^2 g\,R_2^4}{8\,\eta_a}\right) \times \left(1 - b^4 - \frac{(1 - b^2)^2}{\ln(1/b)}\right) \tag{17}$$

By substituting the dimensions of the stirring chamber in Equation 17, then

$$Q_m = 0.068/\eta_a \tag{18}$$

Equation 17 is represented in Fig. 5 for different values of R_1 and R_2, i.e. different gap widths between the stirrer and the stirring chamber. The figure shows that the flow rate Q_m increases with decreasing apparent viscosity η_a, and at the same value of η_a, Q_m is lower for a smaller gap width.

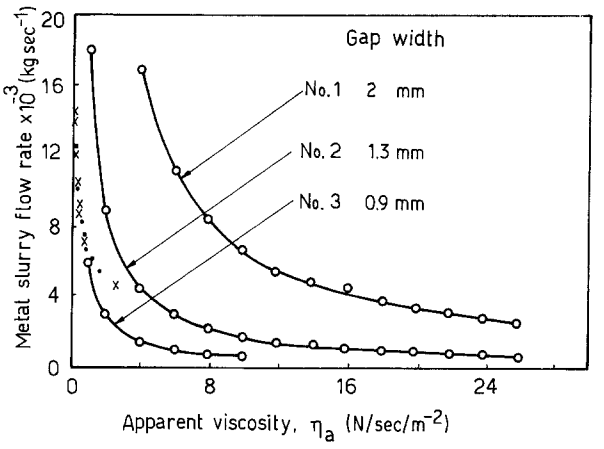

Figure 5 Calculated and experimental relationships between slurry flow rate and apparent viscosity for different exit gap widths.

5.2. Other factors affecting port flow rate

In the case of continuous rheocasting, the exit port area (Section B in Fig. 1) is an additional factor for controlling Q_p. If B is greater than or equal to A (the gap cross-sectional area), no blocking for the flow will occur. Therefore, the value of flow rate across B (Q_p) will be similar to that across A (Q_m) calculated from Equation 17. On the other hand if B is less than A, a case of flow blocking will occur, which results in a Q_p value less than Q_m. If a reduction in the flow rate Q_m is required, the exit port should be set at a cross-sectional area B smaller than the gap cross-sectional area A.

Equation 5 was applied to calculate the slurry apparent viscosity of Bi–17 wt % Sn alloy slurry at the exit port during continuous rheocasting. The metal flow rate Q_p was measured experimentally and the results of Q_p against η_a are plotted in Fig. 6. The figure shows that Q_p decreases sharply initially and then gradually with increasing η_a, similarly to the theoretically calculated curves. A comparison between theoretical and experimental results indicates that the experimentally determined flow rate values are less than the calculated ones for a gap width of 2 mm (the present

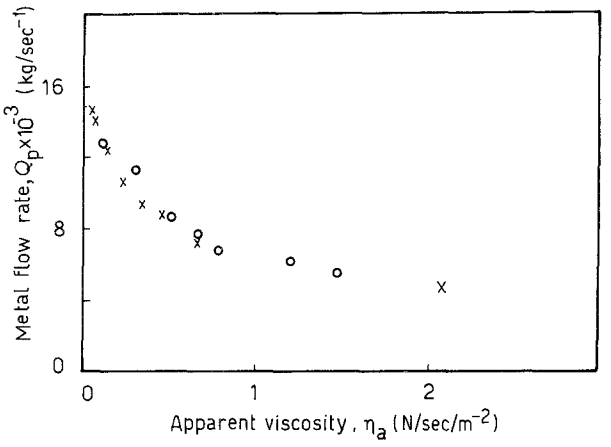

Figure 6 Experimental flow rate against apparent viscosity of slurry at the exit port at two values of γ: (○) 270, (×) 900 sec^{-1}.

rheocaster). This is in agreement with the present experimental set-up where B was less than A. The figure shows that B corresponded to the range of 0.9 to 1.3 mm width.

6. Conclusions

From the above analysis the following conclusions can be drawn:

1. The apparent viscosity (η_a) of Bi–17 wt % Sn slurry is dependent on the volume fraction of solid (G_s) and the shear rate (γ), following the relationship

$$\eta_a = 0.34 \exp (13.08\ G_s)\ \gamma^{-0.6}$$

2. The steady-state torque is found to be dependent on stirring speed, gap dimensions and apparent viscosity following the relationship

$$M = \text{Constant} \times \omega_i \left(\frac{b}{1 - b^2}\right)^{0.6} \int_0^h \eta_a\, dz$$

3. The maximum flow rate at the exit port is found to be dependent on pressure head, gap dimensions and apparent viscosity following the relationship

$$Q_m = \left(\frac{\pi \varrho^2 g R_2^4}{8\ \eta_a}\right)\left[1 - b^4 - \frac{(1 - b^2)^2}{\ln(1/b)}\right]$$

Appendix: Derivation of torque equation

The relationship between the shear stress τ and the shear rate γ (Equation 1) can be written in the following form:

$$\gamma = f(\tau)$$

Also

$$\gamma = r \frac{d\omega_i}{dr} \tag{A1}$$

Then

$$\frac{d\omega_i}{dr} = \left(\frac{1}{r}\right) f(\tau)$$

and

$$d\omega_i = \left(\frac{1}{r}\right) f(\tau)\, dr \tag{A2}$$

By integration

$$\omega_i = \int_{r_i}^{r_0} \left(\frac{1}{r}\right) f(\tau)\, dr \tag{A3}$$

Since the apparent viscosity η_a is a function of G_s, which is again a function of the height of the stirring chamber, L, due to the applied temperature gradient, then η_a is also a function of L.

For an element Δz along the height L (Fig. 1), the incremental shear stress τ is given by

$$\tau = \left(\frac{dM}{dz}\right)\left(\frac{1}{2\pi r^2}\right) \tag{A4}$$

where dM is the incremental torque, and r is the radius. As

$$\tau r^2 = \text{Constant}$$

therefore

$$\tau_i R_i^2 = \tau_0 R_0^2$$

then

$$\tau_0 = \tau_i \left(\frac{R_i}{R_2}\right)^2 \tag{A5}$$

By differentiating Equation A4,

$$d\tau = -2\left(\frac{dM}{2\pi dz}\right)\left(\frac{dr}{r^3}\right) \tag{A6}$$

Dividing Equation A6 by A4, then

$$\frac{d\tau}{\tau} = -2\frac{dr}{r}$$

$$dr/r = -\frac{1}{2}\left(\frac{d\tau}{\tau}\right) \tag{A7}$$

Substituting in Equation A3, then

$$\omega_i = \frac{1}{2}\int_{\tau_0}^{\tau_i} \left(\frac{f(\tau)}{\tau}\right) d\tau \tag{A8}$$

In Equation A8, τ describes the variation of shear stress along the height of the stirring chamber and can be replaced by $\tau(z)$. The theoretical treatment of $\gamma = f(\tau)$ has been considered by previous investigators [18, 22] and it was found to be very complicated. Some other investigators tried to treat it on a semi-empirical basis [14]. In the present work, an approach based on the experimental measurements of flow curves is applied and the following relationship can be written (see Equation 4):

$$\gamma = \left(\frac{\tau}{k}\right)^{1/n}$$

By substituting in Equation A8, then

$$\omega_i = 0.5 \int_{\tau_0(z)}^{\tau_i(z)} \left(\frac{\tau^{1/n}}{k^{1/n}\tau(z)}\right) d\tau$$

and

$$\omega_i = \frac{n\ \{\tau_i(z)^{1/n} - [b_1 \tau_i(z)]^{1/n}\}}{2k^{1/n}}$$

where $b_1 = (R_1/R_0)^2$. Then

$$\tau_i(z) = \frac{(2\omega_i)^n\ k}{n^n\ (1 - b_1^{1/n})^n}$$

Applying Equation A4 to calculate the torque induced in the stirrer, then

$$\tau_i(z) = \left(\frac{dM}{dz}\right) 0.5\pi R_i^2$$

and

$$M = \int_0^h \tau_i(z)\, 2\pi R_i^2\, dz$$

$$M = 5.65 \times 10^{-3}\, \omega_i^n \int_0^h K\, dz$$

$$M = 1.92 \times 10^{-3}\, \omega_i^n \int_0^h \exp(13.08\, G_s)\, dz \qquad \text{(A9)}$$

Substituting the value of G_s given in Equation 2 in Equation A9,

$$M = 1.92 \times 10^{-3} \omega_i^n \int_0^h \exp\left(\frac{13.08(486 - T)}{534.5 - T}\right) dz \qquad \text{(A10)}$$

Equation A10 includes a term for the temperature distribution along the axial direction. The function $T = f(z)$ has been calculated using the heat flow model as well as experimental measurements, where the results are found to be similar. From these results a straight-line relationship between the absolute temperature T and the axial coordinate z is obtained as follows:

$$T = 486 - Sz \qquad \text{(A11)}$$

where S is the slope of the straight line. By substituting in Equation A10, then

$$M = 1.92 \times 10^{-3} \omega_i^n \int_0^h \exp\left(\frac{13.08\, Sz}{48.5 + Sz}\right) dz \qquad \text{(A12)}$$

Acknowledgements

The authors acknowledge financial support by the Egyptian Student Mission and Giesserei-Institut der RWTH, Aachen, at which the experimental part of this work was done. They wish to thank Professor A. S. El-Sabagh of Ain Shams University, Egypt and Professor Peter R. Sahm of Giesserei-Institut, Aachen, FRG, for their contribution.

References

1. R. MEHRABIAN and M. C. FLEMINGS, *Trans. Amer. Foundrymen's Soc.* **80** (1972) 173.
2. *Idem. Die Cast. Eng.* (July–August 1973) 49.
3. E. F. FASCETTA, R. G. RIEK, R. MEHRABIAN and M. C. FLEMINGS, *ibid.* (September–October 1973) 44.
4. *Idem, Amer. Foundrymen's Soc., Cast Met. Res. J.* **9** (1973) 167.
5. *Idem, Trans. Amer. Foundrymen's Soc.* **81** (1973) 95.
6. D. B. SPENCER, R. MEHRABIAN and M. C. FLEMINGS, *Metall. Trans.* **3** (1972) 1925.
7. R. G. RIEK, A. VRANCHNOS, K. P. YOUNG, N. MATHUMOTO and R. MEHRABIAN, *Trans. Amer. Foundrymen's Soc.* (1975) 25.
8. M. C. FLEMINGS and R. MEHRABIAN, *ibid.* **81** (1973) 81.
9. R. MEHRABIAN and M. C. FLEMMINGS, in Proceedings of American Society for Metals Seminar on New Trends in Materials Processing, October 1974.
10. *Idem,* "New Trends in Materials Processing" (American Society for Metals, Metals Park, Ohio, 1975).
11. R. MEHRABIAN, A. SATO and M. C. FLEMINGS, *Light Metals* **2** (1975) 177.
12. R. G. RIEK, K. E. YOUNG and M. C. FLEMINGS, *Mater. Sci. Eng.* **25** (1976) 103.
13. M. C. FLEMINGS and R. MEHRABIAN, "New trends in Materials Processing" (American Society for Metals, Metal Park, Ohio, 1976) p. 98.
14. P. A. JOLY and R. MEHRABIAN, *J. Mater. Sci.* **11** (1976) 1393.
15. F. J. KIEVITS and K. V. PRABHAKAR, in Proceedings of International Symposium on Quality Control of Engineering Alloys and the Role of Metal Science, Delft University, 1977, pp. 203–213.
16. A. M. ASSAR, N. A. EL-MAHALLAWY and M. A. TAHA, *J. Mater. Sci.* in press.
17. R. S. SMEULDERS, PhD thesis, Delft University (1984).
18. D. QUEMADE, *Rheol. Acta* **17** (1978) 632.
19. V. LAXMANN and M. C. FLEMINGS, *Met. Trans.* **11A** (1980) 1927.
20. S. D. E. RAMATI, G. J. ABBASCHIAN and R. MEHRABIAN, *ibid.* **9B** (1978) 241.
21. A. BENDIJK and L. KATGERMAN, Internal Report, Laboratorium voor Metaalkunde, Delft University (1977).
22. N. A. FRANKEL and A. ACRIVOS, *Chem. Eng. Sci.* **1** (1967) 22.

Received 28 May
and accepted 17 August 1987